

Analysis of the DWT Characteristics of MR Molecular Images Obtained by Using MNPCA

*Junhaeng Lee ^{Ph.D}

Received: 21 May 2018 / Accepted: 20 July 2018 / Published online: 1 September 2018

©The Author(s) 2018


Abstract- I was suggested a method to analyze the DWT(discrete wavelet transform) characteristics of magnetic resonance(MR) molecular images obtained by using contrast agent made of magnetic nanoparticles. The magnetic nanoparticles contrast agents(MNCA) were prepared by thermal decomposition method. We transplanted gastric cancer stem cells into experimental mice four weeks before the experiment. After injecting MNCA into the prepared mice, the MR molecule images were obtained as follows: before to MNCA injection, immediately after MNCA injection, 2 hours after MNCA injection and 4 hours after MNCA injection. At this time, we were used pulse sequence which T₂ TSE, T₂ MPGR, T₂^{*}, and UTE. We extracted and analyzed the signal characteristics of the pulse sequence of MR molecular images obtained by MNCA. The characteristics between T₂ signal (T₂ MPGR, T₂ TSE, T₂^{*}) and UTE (Ultra short TE) were extracted and compared. Feature extraction for each signal was performed by the DWT method. The M program for DWT 3-step decomposition was used the MATLAB Toolbox. After decomposing in 3-step, we extracted the horizontal low frequency (A4H), vertical low frequency (A4V), horizontal high frequency (H4V), vertical high frequency (V4H), horizontal diagonal high frequency (D4H) and high frequency (D4V).

The extracted features were compared and analyzed for each pulse signals. The results of this study can be used to demonstrate the effectiveness of MNCA for the usefulness of MR molecular imaging and UTE signals.

Keyword: Image processing, Discrete Wavelet Transform, MR pulse sequence, T₂ Weighted Image, MR Molecular Imaging, Magnetic nanoparticles

I. Introduction

Nowadays, medical scientists have been clearly analyzed to diagnose of disease through change of in molecular level which of fundamental stages of disease, it is effort to develop the nano medical technology for predict outcomes of disease treatment. The age of precision medicine is approaching with the convergence of medical science and nanotechnology, precision medicine is a technology that enables to diagnosis and treat using bio compatible nano-bio chip, nano robot, and so on. Nanotechnology has also been applied to the field of medical imaging, enabling to the acquisition of molecular imaging. Molecular imaging is enable to early diagnosis for recognizing changes in

J. Lee 

*Junhaeng Lee ^{Ph.D}

Department of Radiology, Nambu University, 62271,
Gwangju, Republic of Korea

*corresponding author

the cellular level prior to developing of disease, also, it is can predict the prognosis after treatment [1-3]. Positron emission tomography (PET), Magnetic resonance imaging (MRI), and Computed tomography (CT) are widely used as imaging modality for molecular imaging. Among these imaging modality, PET has excellent sensitivity and specificity, but it has disadvantages of using radioisotope and low spatial resolution and tissue contrast [4-5]. MRI devices have the advantage of acquiring images with high resolution and tissue contrast without using ionizing radiation [6-13]. However, it has disadvantage that acquisition process of the signal is relatively longer than Computed tomography. The development of nanotechnology for MR molecular imaging is active in the field of nano contrast agent. In this study, we propose a novel imaging method through conventional T2 weighted imaging (T2W), Ultra short TE (UTE) using a nano contrast agents. The features are extracted and compared to between conventional T2 (T2 MPGR, T2 TSE, T2 STAR) and Ultra short TE (UTE) for evaluate the efficiency of the proposed UTE pulse sequence. Feature extraction is performed by the DWT (Discrete wavelet transform) method, it is a method of decomposing a signal into a set of base functions such as Fourier transform. The program for the DWT three-step decomposition was used in the MATLAB Tool Box. After decomposing in three steps, the feature of the components of horizontal low frequency (A4H), vertical low frequency (A4V), horizontal high frequency (H4V), vertical high frequency (V4H), horizontal diagonal high frequency (D4H), vertical diagonal high frequency (D4V) in the low frequency region were extracted. The results of this study can be used to demonstrate the efficiency of the nano-contrast agent for MR imaging and the utility of the UTE signal.

II. Materials and Methods



A. Materials

Polysorbate 80 (P80), ethylenediamine, 1,4-dioxane (99.8%), and 1,1'-carbonyldiimidazole (CDI) were purchased from Sigma Aldrich Chemical Co. Phosphate buffered saline (PBS: 10 mM, pH 7.4), Roswell Park Memorial Institute-1640 (RPMI-1640), fetal bovine serum (FBS) and antibiotic-antimycotic solution were purchased from Gibco and dialysis membrane (1 kDa MWCO) from Spectrum laboratory. Hyaluronic acid (1 MDa) was supplied from Yuhan Pharmaceutical Corporation (Seoul, Korea). MKN-45 (American Tissue Type Culture) cell line was grown in medium containing 10% FBS and 1% antibiotic antimycotic at 37°C and a humidified 5% CO₂ atmosphere. Ultrapure deionized water was used for all of the syntheses.

B. Methods

1. Synthesis of magnetic nanoparticles contrast agent

The magnetic nanoparticles contrast agents (MNCA) were prepared by thermal decomposition method. Briefly, 2 mmol iron (III) acetylacetonate, 1 mmol manganese (II) acetylacetonate, 10 mmol 1,2-hexadecanediol, 6 mmol dodecanoic acid, and 6 mmol dodecylamine were dissolved in 20 mL benzyl ether under an ambient nitrogen atmosphere. The mixture was then preheated to 200 °C for 2 h and refluxed at 300 °C for 30 min. After the reactants were cooled to room temperature, the products were purified with an excess of pure ethanol. Approximately 11 nm MNCA were synthesized using the seed-mediated growth method.

2. Feature Extraction on Image by DWT

The Discrete Wavelet Transform (DWT) is converted

the signal from the spatial domain to the frequency domain. The human eye is more sensitive to the information of the low frequency component than the high frequency component [15]. Thus, DWT is used for JPEG compression algorithms, boundary detection, and to extract texture information from an image. It is also used for contour extraction by using the conversion coefficients of low frequency and medium frequency components most sensitive to contour information among DWT coefficients [16]. In order to solve the disadvantage of STFT's fixed resolution, wavelet transform is performed by applying a short window to the high-frequency band in the time-frequency plane to increase the temporal resolution. In the low-frequency range, the frequency resolution can be increased by applying a long window [17-19]. The wavelet transform introduced by Ingrid Daubechies and Stephane Mallat is a method of decomposing the signal into a set of basis functions such as Fourier transform [17]. However, unlike Fourier transform, wavelets, which are band-pass signals with local energy concentration, are used as basis functions. These wavelets can be obtained by extending and moving a single prototype wavelet called a mother wavelet. The wavelet transform refers to an expansion factor that is several times larger than the frequency of the extended signal, and this factor is called the scale. At this time, a value of scale is mainly used as a multiple of 2^n [20]. As the scale increases, the spatial resolution of the wavelet transform signal is decreases at a given scale and appear the low frequency components [20]. The wavelet transform is obtained to $\Psi(x)$ by dilating / translating the circular wavelet in Equation. (1) [19].

$$\Psi_{a,b}(x) = \frac{1}{\sqrt{\alpha}} \Psi\left(\frac{x-b}{\alpha}\right) \quad (\text{Equation 1})$$

Herein, α is scaling coefficient, β is translation coefficient. And $\alpha^{-1/2}$ is normalization factor, if $\alpha < 1$, high-frequency wavelet having a small width on the time axis, if $\alpha > 1$, it is a wide-frequency wavelet. The shape of the wavelet varies according to the proposed person, Application areas differ depending on the characteristics and advantages of each wavelet. The two-dimensional signal decomposed on an orthonormal basis is decomposed into spatially directional frequency components as shown in Equation. (2) [19].

$$\begin{aligned} A_{2^{m+1}f} &= \sum_{k=1}^K \sum_{l=1}^L h(2m-k) h(2n-l) A_{2^m f} \\ H_{2^{m+1}f} &= \sum_{k=1}^K \sum_{l=1}^L h(2m-k) g(2n-l) A_{2^m f} \\ V_{2^{m+1}f} &= \sum_{k=1}^K \sum_{l=1}^L g(2m-k) h(2n-l) A_{2^m f} \\ D_{2^{m+1}f} &= \sum_{k=1}^K \sum_{l=1}^L g(2m-k) g(2n-l) A_{2^m f} \end{aligned} \quad (\text{Equation 2})$$

In equation (2), h is transfer function of the decomposition low pass filter, g is transfer function of the decomposition high pass filter. [Figure. 2] showed decomposition and synthesis of two-dimensional signals by DWT, [Figure. 2] (a) is the decomposition process of the 2-D discrete approximate signal and [Figure. 2] (b) is a block diagram of the synthesis process. [Figure. 2] (c) shows the coefficient matrix of the two-dimensional signal decomposed into multiple resolutions, That is, a coefficient matrix that is two-level decomposed into packets of frequency component having spatial directionality, [Figure. 2] (c), VH1 means a coefficient matrix of vertical high-frequency components decomposed at level 1, HH1 and DH1 mean the coefficient matrix of the horizontal high-frequency component and the diagonal high-frequency component, respectively.

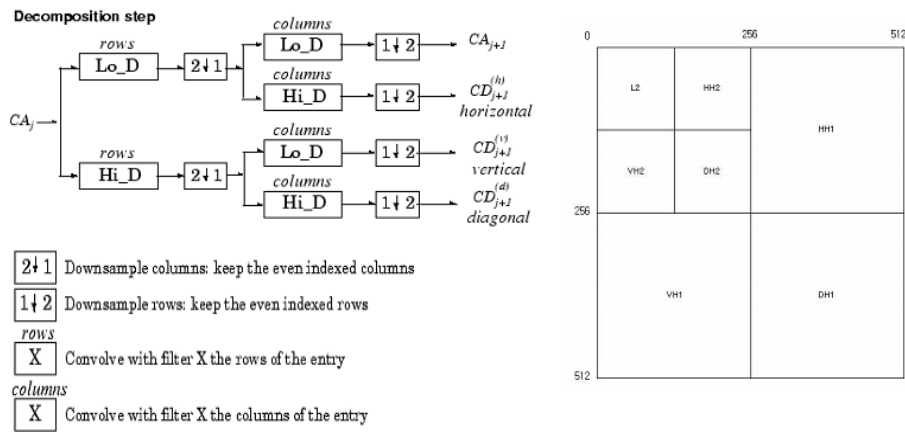


Figure 2. Decomposition and synthesis of two-dimensional signals by DWT

III. Experiments and results

A. Schematic illustration

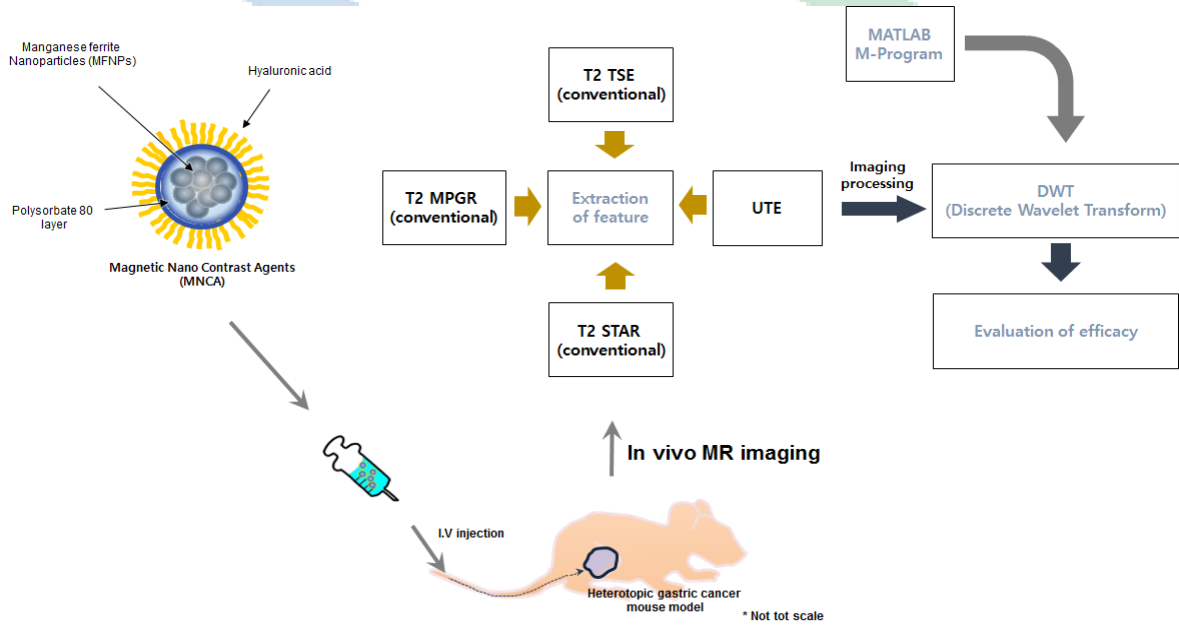


Figure 3. Preparing the experimental model

As shown in figure 3, the experiment was designed and proceeded after injecting the synthesized contrast

agent into the body of a mouse. The obtained MR images (T2 TSE, T2 MPGR, T2 STAR, UTE) were compared and analyzed by the proposed image technique in this paper.

B. Acquisition of MR Molecular Imaging

All animal studies were approved and accredited by the Association for Assessment and Accreditation of

Laboratory Animal Care (AAALAC) International. Six-week-old female nude mice were injected intravenously with an anesthetic Zoletil / Rompun mixture. After anesthesia, the mice were injected to 1.0×10^7 gastric cancer cells which after dispersing in 200 mL of saline solution into thighs. And then, MR imaging were obtained on the 5th week after transplanting the gastric cancer cell line. MR imaging was performed with 3 T SIMENS clinical instruments using a wrist coil. Imaging was performed as follows: Pre-contrast, Immediate (IMM), 2 h after (2H), and 4 h after (4 h) imaging as shown table 2. (Table 1 : MR parameter, Figure. 4 : pulse diagram)

Table -1. Sequence (3T SIEMENS)

	FOV read	FOV phase	Slice Thickness	TR	TE
T2 MPGR	100 mm	87.5 %	1.50 mm	594 ms	15.0 ms
T2 TSE	100 mm	80.4 %	1.00 mm	4140 ms	113 ms
T2 STAR	100 mm	100 %	1.00 mm	14.85 ms	5.85 ms
UTE	110 mm	100 %	0.57 mm	6.72 ms	0.07 ms

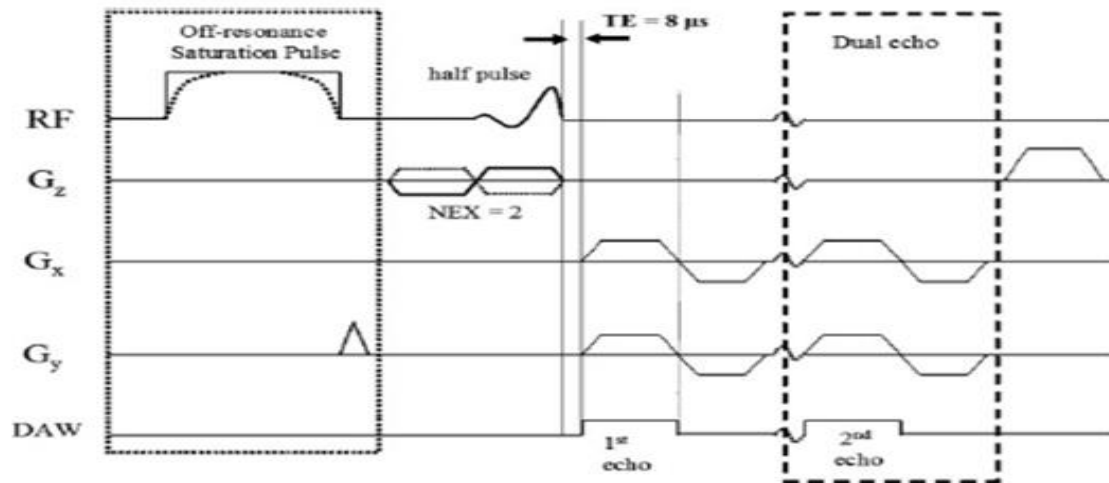

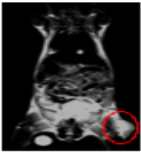
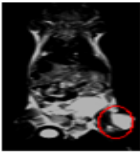




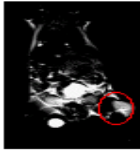





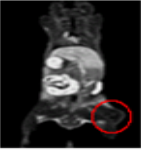

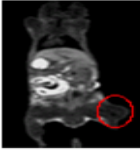


Figure 4. Pulse sequence

Table-2. Molecular MR Imaging of CD44-expressed Gastric Cancer in Mice using T2 and Ultra Short TE Pulse

Sequences

	Pre	IMM	After 2H	Afetr 4H
T2 MPGR MRI				
T2 TSE MRI				
T2 star MRI				
UTE MRI				

C. Feature Extraction

The region of the stomach cancer cells in the acquired image was set as the region of interest (ROI). The separated images were adjusted in the form of 256 x

256 pixels for the same experiment with MATLAB Tool Box, the number of bits per pixel was adjusted to 8 bits. The experimental procedure was performed in the order of Figure 5.

Table 3. Feature parameters of coefficient matrix.

Abbreviation	Meaning of feature extraction parameter
A4H	low frequency coefficient matrix (horizontal direction)
A4V	low frequency coefficient matrix (vertical direction)
H4V	horizontal high-frequency coefficient matrix
V4H	vertical high-frequency coefficient matrix
D4H	diagonal high frequency coefficient matrix (horizontal direction)
D4V	diagonal high frequency coefficient matrix (vertical direction)

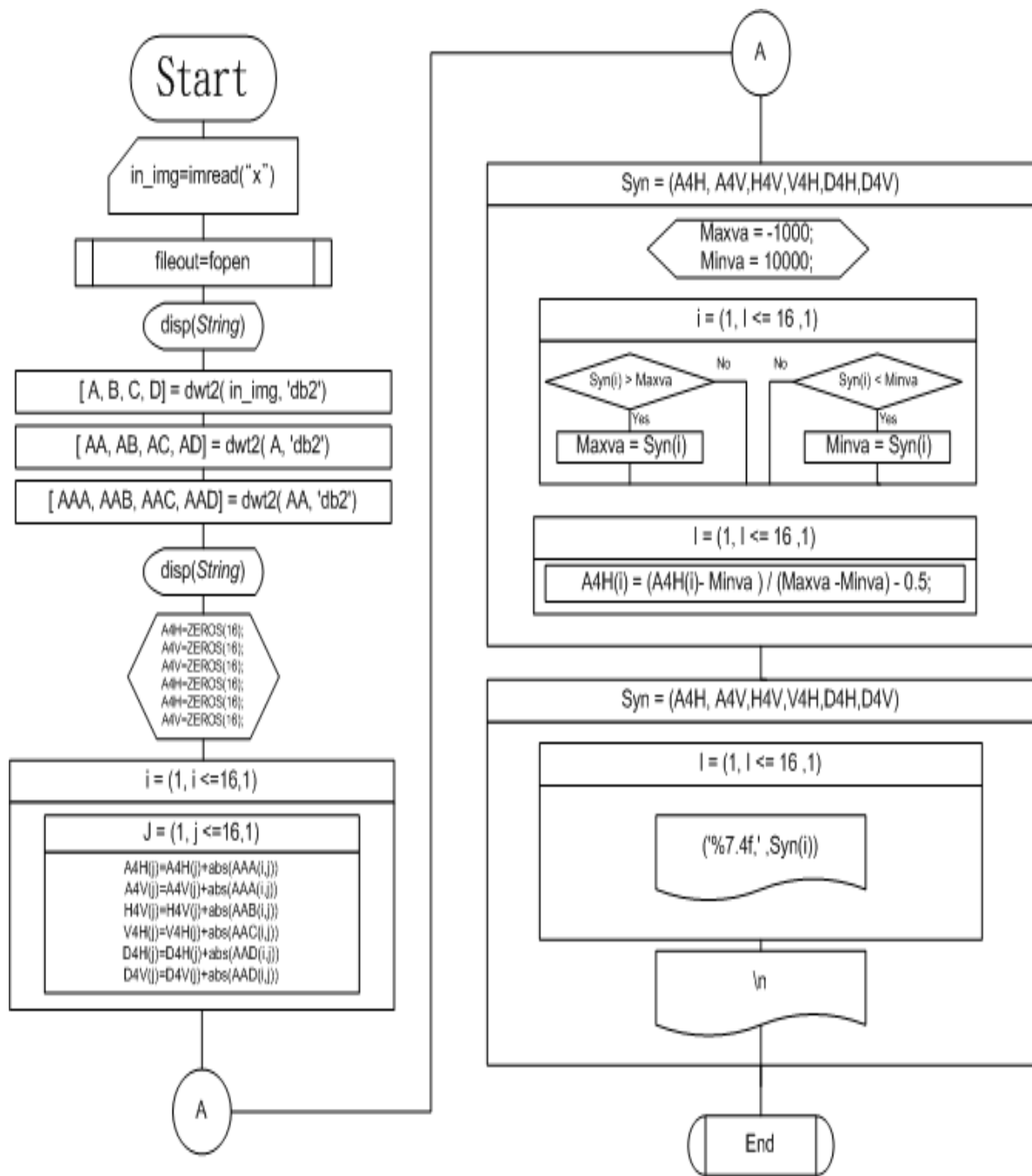


Figure 5. Feature Extraction Flow chart

D. Results of DWT

The results of the T2 MPGR MR image, the T2 TSE

MR image, the T2 star MR image, and the UTE image DWT obtained by the program execution are shown in Table 5.

Table-4. DWT results of T2 MPGR MRI







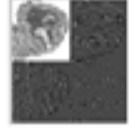
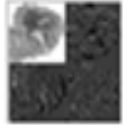




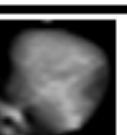
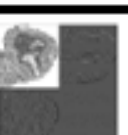
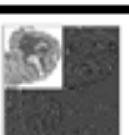
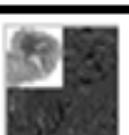
		ROI	DWT		
		Image	1 Level	2 Level	3 Level
T2 MPGR	Pre				
MR image	IMM				
	2H				
	4H				

Table-5. DWT results of T2 TSE MRI

















		ROI	DWT		
		Image	1 Level	2 Level	3 Level
T2 TSE	Pre				
MR image	IMM				
	2H				
	4H				

Table-6. DWT results of T2 star MRI






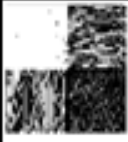










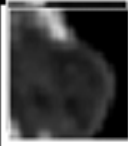



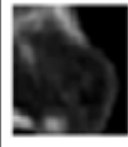











		ROI	DWT		
		Image	1 Level	2 Level	3 Level
T2 star	Pre				
MR image	IMM				
	2H				
	4H				

Table-7. DWT results of UTE MRI

		ROI	DWT		
		Image	1 Level	2 Level	3 Level
UTE	Pre				
MR image	IMM				
	2H				
	4H				

IV. Conclusion and discussion

Nanotechnology using magnetic resonance imaging (MRI) devices has led to active development of nano-contrast agents. The aim of this study was to evaluate the usefulness of T2 signals and UTE signals in molecular MR images obtained after injection of nanoparticle agents into mice which of gastric cancer

expressing CD44.

A. Pre-Injection

T2 pulse sequence and UTE signal before injection of contrast agent showed similar frequency change in horizontal low frequency signal, vertical low frequency signals showed only different UTE signals. Horizontal high frequency, vertical high frequency, and diagonal high frequency were high frequency

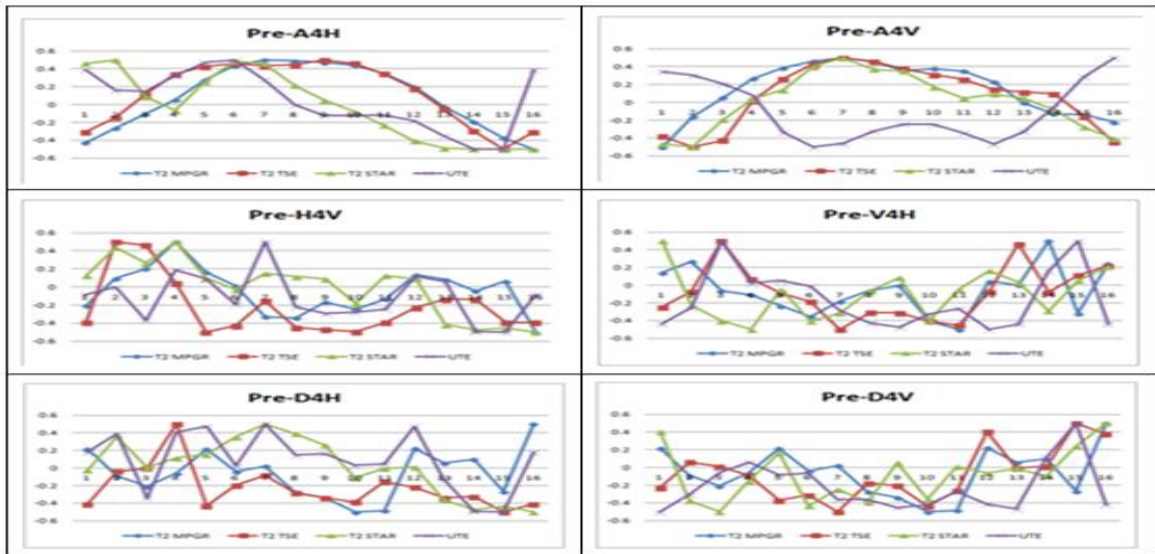


Figure 6. Analysis of signal in low frequency region after 3 Level DWT before contrast agent Injection.

B. Injection Immediately

Immediately after injecting the contrast agent, the T2 pulse sequence and the UTE signal showed similar frequency changes in the horizontal low frequency signals, vertical low frequency signals are different

from UTE signal and T2 MPGR image only. The horizontal high - frequency component showed no change only in T2 MPGR component, vertical high frequency, each diagonal high frequency showed high frequency.

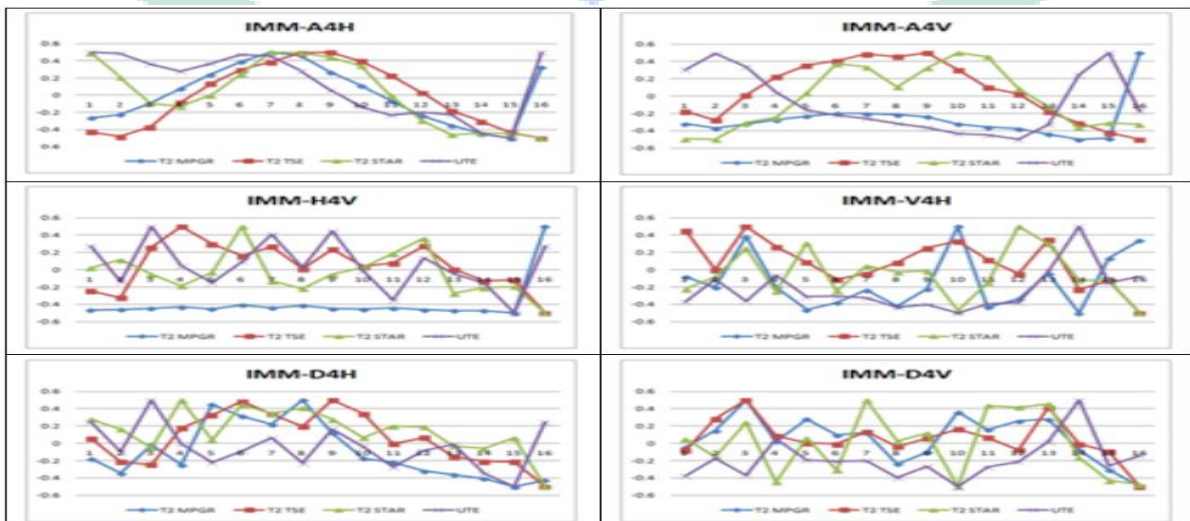


Figure 7. Analysis of signal in low frequency region after 3 Level DWT immediately after injection of contrast agent.

contrast agent.

C. After 2h of Injection

The T2 pulse sequence and the UTE signal in the acquired image 2 hours after the injection of the contrast agent showed the similar frequency change in the horizontal low frequency signal, vertical low

frequency signals showed only different UTE signals. The horizontal high - frequency component showed no change only in T2 MPGR component, vertical high frequency, each diagonal high frequency showed high frequency

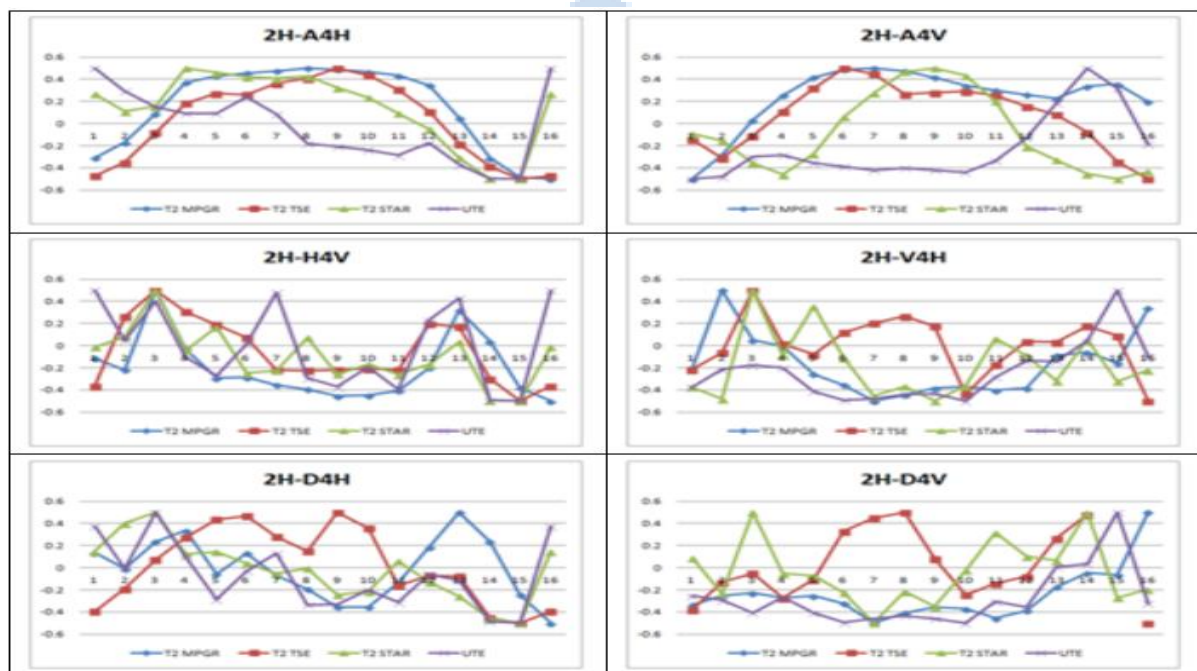


Figure 8. Analysis of signal in low frequency region after 3 Level DWT 2 hours after injection of contrast agent.

D. After 4h of Injection

The T2 pulse sequence and the UTE signal were different from the T2 MPGR signal in the horizontal low frequency signal in the acquired image 4 hours after contrast injection. The remain of the signal appeared in a similar form, vertical low frequency

signals differ only in T2 MPGR and UTE signals.

The horizontal high - frequency component showed no change only in T2 MPGR component, vertical high frequency, each diagonal high frequency showed high frequency

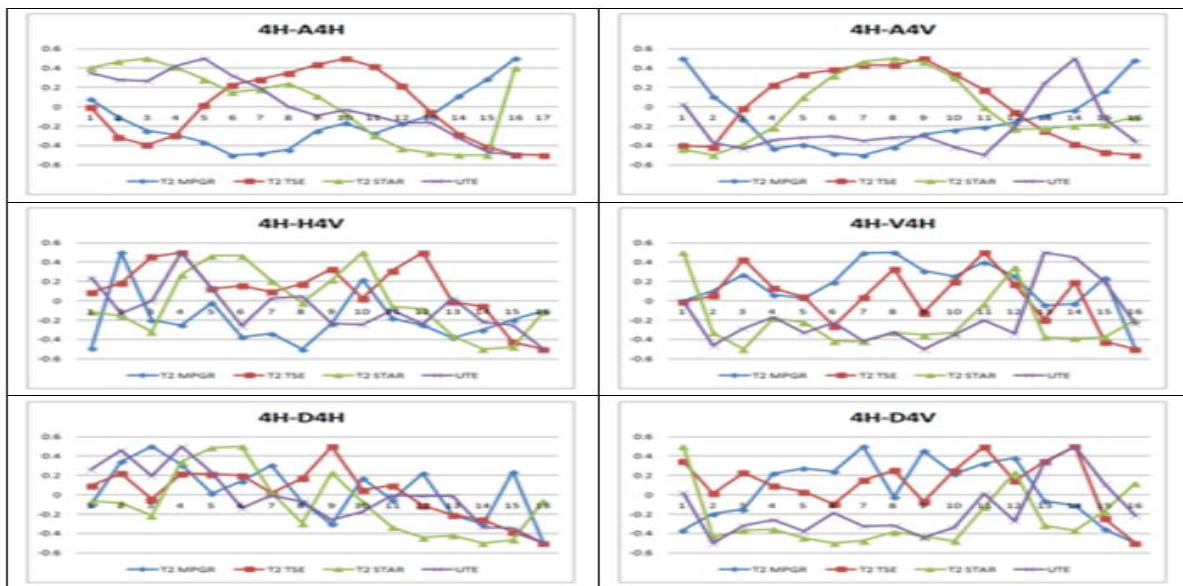


Figure 9. Analysis of signal in low frequency region after 3 Level DWT 4 hours after injection of contrast agent.

The UTE pulse sequence is a combination of the characteristics of T2-weighted images that well represent pathologic changes and the characteristics of T1-weighted images that well represent anatomical structures, it is also used as a method to reduce image distortion caused by motion. As a result of analyzing the characteristics of each signal, it is found that in the low frequency region after the 3-level DWT corresponding to the frequency axis of the K-space, the vertical low frequency component in the low frequency region after the 3-level DWT corresponding to the phase axis of the K- is proportional to TR and TE. The reason why the vertical low-frequency component in the signal before the injection of contrast agent is low in UTE is interpreted as a result of the short signal due to the short TR. Vertical low-frequency components at 2 and 4 hours after injection of contrast medium were lower in T2 MPGR and UTE signals, the reason for this is interpreted as a phenomenon resulting from a small amount of signal

emission due to a small number of excited TRs. The horizontal high frequency component and the vertical high frequency component after the 3-level DWT were similar patterns in T2 star and UTE. This is also interpreted as a phenomenon that occurs because the acquisition of T2 star and UTE images is similar to TR and TE. As a result, it was found that the T2 signal and the UTE signal are proportional to TR and TE. Therefore, acquisition of MR molecular image using UTE signal should increase tissue resolution by using nano contrast agent.

Competing interests

The authors declare that there is no conflict of interest regarding the publication of this paper

IV. Reference

- [1] Mahwood U, Emerging Technologies That Will Change the World : Molecular Imaging. Tech Rev, Vol.

106, 2003.

[2] Chang, Thomas Ming Swi, "Artificial cells", World Scientific Publishing. co. Pte. Lte, 2007.

[3] Byeong-Chole Ahn, Applications of molecular imaging in drug discovery and development process, Curr Pharm Biotechnol, Vol. 12, No. 4, pp.459-468, 2011.

[4] Ho-Taek Song, Jin-Suck Suh, Cancer -Targeted MR Molecular Imaging, J Korean Med Assoc, Vol. 52, pp.121-124, 2009.

[5] Gilad AA, McMahon MT, Walczak P, Winnard PT Jr, Raman V, van Laarhoven HW, Skoglund CM, Bulte JW, van Zijl PC., Artificial reporter gene providing MRI contrast based on proton exchange, Nat Biotechnol., Vol. 25, pp.217-219, 2007.

[6] A. Yoshitaka, T. Ichkawa, A survey on content-based retrieval for multimedia databases, IEEE Transaction on Knowledge and Data Engineering., Vol. 11, No. 1, 1999.

[7] Jaemoon Yang, Eun-Kyung Lim, Hong Jae Lee, Joseph Park, Sang Cheon Lee, Kwangyeol Lee, Ho-Geun Yoon, Jin-Suck Suh, Yong-Min Huh, Seungjoo Haam., Fluorescent magnetic nanohybrids as multimodal imaging agents for human epithelial cancer detection., Vol. 20, No. 29, pp.2548-2555, 2008.

[8] Hwunjae Lee, Seung-Hyun Yang, Dan Heo,

Hyeyoung Son, Seungjoo Haam, Jin-Suck Suh, Jaemoon Yang, Yong-Min Huh, J of Nanoscience and Nanotechnology., Vol. 16, pp. 196-202, 2016.

[9] Weissleder R and Mahmood U, Molecular imaging, Radiology., Vol. 219, pp.3160-3330, 2001.)(Herschman HR, Molecular imaging : Looking at problems, seeing solutions, Science., Vol. 302, pp.605-608, 2003.

[10] Britz – Cunningham, SHAdelstein SJ, Molecular targeting with radionuclides, State of the science., Vol. 44, pp.1945-1961, 2003.

[11] Strauss LG, Conti PS, The applications of PET in clinical oncology, J Nucl Med., Vol. 32, pp.623-648, 1991.

[12] Rouze NC, Schmand M, Siegal S, Hutchins GD., Design of a Small Animal PET Imaging System with 1 microliter Volume Resolution, IEEE Trans Nucl Sci., Vol. 51, pp.757-763, 2004.

[13] Jan ML, Chuang KS, Chen GW, Ni YC, Chen S, Chang CH, ET al, A three-dimensional registration method for automated fusion of micro PET-CT_SPECT whole-body images, IEEE Trans Med Imaging., Vol. 24, pp.886-893, 2005.

[14] Joanne E. Holmes, Graeme M. Bydder, MR imaging with ultra short TE (UTE) pulse sequence : Basic Principles, Radiography., Vol. 11, pp. 163-174,

2005

[15] Maint BA, Elsen PA and Veirgever MA., 3D multimodality medical image registration using morphological tools., Image Vis. Comput Vol. 19, p.53-62, 2001.

[16] H. Kauppinen, T. Seppanen, M. Pietikainen, "An experimental comparison of Autoregressive and Fourier-Based Descriptors in 2D shape Classification", IEEE Transaction on PAMI, Vol.17, No.2, pp.201-207, February. 1995.

[17] Sangbock Lee, Junhaeng Lee, Taesil Kim, "Disease Recognition on Medical Images Using

Neural Network", Journal of Korean Society of Radiology, Vol. 3, No. 1, PP. 27~36, 2009.

[18] I. Daubechies, "Orthonormal bases of compactly supported wavelets", Commun. Pure Appl. Math., Vol. 41, No. 7, PP. 909-996, 1988.

[19] Stephane G. Mallat, "A theory for multiresolutional signal decomposition; the wavelet representation", IEEE trans. Pattern Anal. Machine Intell., Vol. 11, No. 7, PP. 674-693, July, 1989.

Ingrid Daubechies, "Ten Lectures on Wavelets", SIAM, 1994.